LPC CAEN

LABORATOIRE DE PHYSIQUE CORPUSCULAIRE

ISMRA - Boulevard Maréchal Juin - 14050 CAEN CEDEX - FRANCE

Formation and decay of hot nuclei in the $^{64}Zn + {}^{nat}Ti$ and $^{36}Ar + {}^{27}Al$ reactions

J.C. Steckmeyer, A. Kerambrun, J.C. Angélique, G. Auger, G. Bizard, R. Brou, C. Cabot,

Y. Cassagnou, E. Crema, D. Cussol, D. Durand, Y. El Masri, P. Eudes, M. Gonin, K. Hagel, Z.Y. He,

S.C. Jeong, C. Lebrun, R. Legrain, J.P. Patry, A. Péghaire, J. Péter, R. Régimbart, E. Rosato, F. Saint-Laurent,

B. Tamain, E. Vient, R. Wada

March 1995 LPCC 95-04

Contribution given at the XXXIIIrd International Winter

Meeting on Nuclear Physics, Bormio, Italy, 23-28 january 1995.

INSTITUT NATIONAL
DE PHYSIQUE NUCLEAIRE ET DE PHYSIQUE DES PARTICULES

CENTRE NATIONAL DE LA RECHERCHE SCIENTIFIQUE

INSTITUT DES SCIENCES
DE LA MATIERE ET DU RAYONNEMENT

UNIVERSITÉ DE CAEN

Téléphone : 31 45 25 00
Télécopie : 31 45 25 49

FORMATION AND DECAY OF HOT NUCLEI IN THE $^{64}Zn + ^{nat}Ti$ AND $^{36}Ar + ^{27}Al$ REACTIONS *

J.C. Steckmeyer [1], A. Kerambrun [1], J.C. Angélique [1], G. Auger [2], G. Bizard [1], R. Brou [1], C. Cabot [2], Y. Cassagnou [3], E. Crema [2], D. Cussol [1], D. Durand [1], Y. El Masri [4], P. Eudes [5], M. Gonin [6], K. Hagel [6], Z.Y. He [1], S. C. Jeong [1-8], C. Lebrun [5], R. Legrain [3], J. P. Patry[1], A. Péghaire [2], J. Péter [1], R. Régimbart [1], E. Rosato [7], F. Saint-Laurent [2], B. Tamain [1], E. Vient [1] and R. Wada [6]

1) LPC, ISMRA, IN2P3-CNRS, Université de Caen, 14050 CAEN CEDEX, France.
2) GANIL , BP 5027, 14021 CAEN CEDEX, France.
3) CEA-DAPNIA/SPhN, CE Saclay, 91191 GIF SUR YVETTE CEDEX, France.
4) FNRS, IPN, UCL, 1348 LOUVAIN-LA-NEUVE, Belgium.
5) SUBATECH, IN2P3-CNRS, 44072 NANTES CEDEX 03, France.
6) Cyclotron Institute, Texas A&M University, COLLEGE STATION, TX 77843, USA.
7) Dipartimento di Scienze Fisiche, Universita di Napoli, 80125 NAPOLI, Italy.
8) Present address : Institute of Nuclear Studies, University of Tokyo, Japan.

Abstract :

The 4π plastic multidetectors installed in the scattering chamber NAUTILUS at GANIL have been used to detect charged products emitted in the reactions of ^{64}Zn with ^{nat}Ti from 35 to 79 MeV per nucleon and of ^{36}Ar with ^{27}Al from 55 to 95 MeV per nucleon. A study of the invariant cross sections in the $V_\perp$ - $V_{//}$ plane reveals three sources of emission at all impact parameters : a high velocity source and a low velocity one (projectile-like and target-like fragments, respectively) as well as a pre-equilibrium component located at intermediate velocities. Fusion-like events are recognized only at the lowest bombarding energies and correspond to a small fraction of the reaction cross-section. The primary mass and excitation energy of the hot nucleus associated to the fast source have been carefully reconstructed from the characteristics of the de-excitation products after separation of both the pre-equilibrium and target emissions. The isotropic emission of particles in the frame of the primary hot nucleus suggests the formation of equilibrated nuclei. The excitation energy increases from peripheral to central collisions, reaching values higher than 10 MeV per nucleon at the highest bombarding energies. Experimental multiplicities and kinetic energy spectra of LCP's and IMF's emitted by the hot nuclei have been compared to statistical and dynamical calculations. For the highest excitation energies, these observables are only accounted for by the incorporation of an isotropic collective expansion of 2. to 2.5 MeV per nucleon.

* Experiments performed at GANIL

1 - INTRODUCTION

With the increase of the excitation energy, the decay of hot nuclei is expected to progressively evolve from a long-lived sequential evaporative process to a fast dissociation of the nuclear source into excited prefragments. One way for a hot nucleus to break up is to undergo a significant initial compression phase followed by an expansion phase towards low nuclear density. Such a scenario is invoked by several theoretical calculations [1-2] : if the excited nuclear system during the expansion phase enters the so-called spinodal region, in which mechanical instabilities can develop, and if it stays long enough in that region, the growth of density fluctuations can lead to a disruption of the nuclear system into fragments [3].

It has also been earlier mentioned that compressional energy is much more efficient than thermal energy to desintegrate a nucleus [4]. As an illustration, the yield of IMF's is well accounted for in the framework of the expanding-evaporating source of ref. [5]. Experimental measurements of radial flow resulting from the expansion phase after initial compression become now available going from a few MeV per nucleon up to more than 10 MeV per nucleon [6-8].

In this paper, we report on the formation and decay properties of hot nuclei formed in the light systems ^{64}Zn on ^{nat}Ti and ^{36}Ar on ^{27}Al at different bombarding energies. In sect. 2, the experimental set-up as well as the event selection are recalled. Sect. 3 deals with the underlying reaction mechanisms involved in the above reactions. In sect. 4 are given experimental results concerning the primary mass and excitation energy of the hot nuclei. These data are compared with various theoretical predictions in sect. 5. We discuss some implications of our results in sect. 6 and our conclusions are given in sect. 7.

2 - EXPERIMENTAL SET-UP AND EVENT SELECTION

2.1. Experimental set-up

The $^{64}Zn + ^{nat}Ti$ system has been measured at several bombarding energies between 35 and 79 MeV per nucleon and the $^{36}Ar + ^{27}Al$ system between 55 and 95 MeV per nucleon.

The experimental procedure can be found elsewhere [9-10]. Charged particles were detected in two plastic multidetectors [11-12] covering a total solid angle of 84% of 4π, between 3 and 150°. Identification of light charged particles (Z = 1 and Z = 2) was achieved for energies above 2.5 MeV per nucleon. For atomic numbers between 3 and 8, their detection was achieved above 2.5 to 5 MeV per nucleon but their identification was possible only above 15 - 20 MeV per nucleon. Heavier fragments were detected and identified in an additional set of seven ΔE-E telescopes between 3 and 30°.

2.2. *Event selection*

In the subsequent analysis only well detected events were kept, those for which more than 60% of the incident momentum (deduced from the parallel momenta of charged products) was collected. Whatever the system and the bombarding energy, these events correspond to a mean total parallel momentum of ~80% of the incident momentum and to a mean total measured charge of 70% of the total charge [9-10].

The data have been sorted as a function of the impact parameter using a global variable : the total transverse momentum defined as the sum of the moduli of the transverse momenta of all charged products detected in an event. Assuming a correspondance between the highest total transverse momenta and the most central collisions, the experimental impact parameter b_{EXP} was deduced from the measured cross sections [9-10]. In these experiments, most of the peripheral collisions have been lost as the projectile-like fragment escaped from the detectors below 3° .

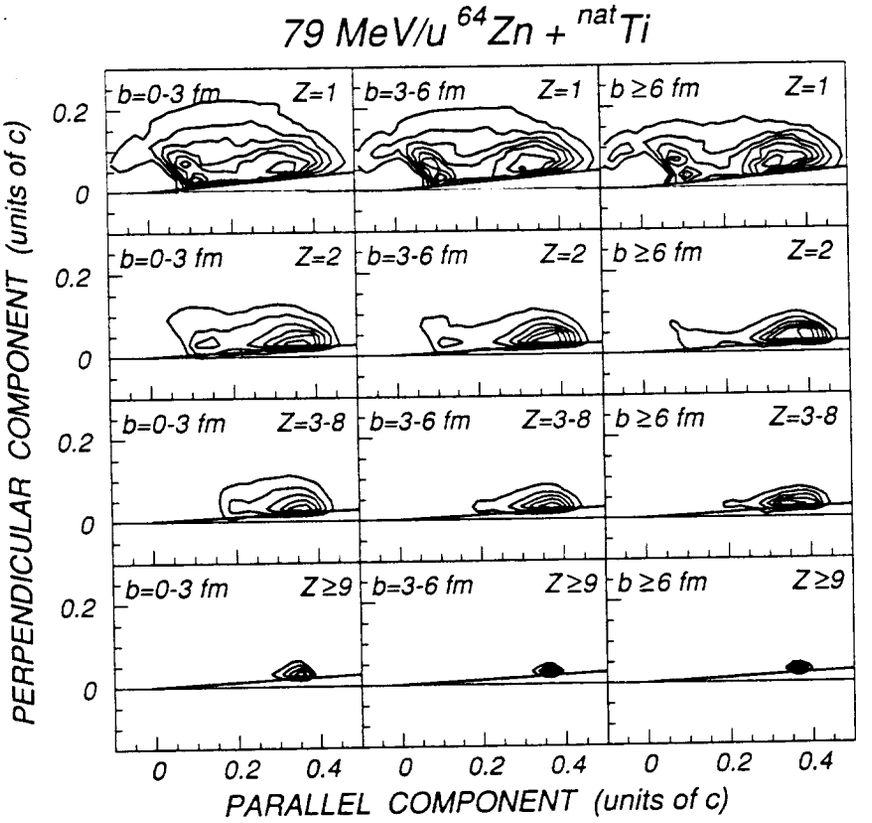

Fig. 1 : Contour plot of the invariant cross-sections $d^2\sigma / V_\perp dV_\perp dV_{//}$ measured in the 79 MeV per nucleon $^{64}Zn+^{nat}Ti$ reactions. The cross sections are given for LCP's (Z=1 and Z=2), IMF's ($3 \leq Z \leq 8$) and heavier fragments ($Z \geq 9$) and for three experimental impact parameter bins.

3 - CHARACTERIZATION OF REACTION MECHANISMS

In fig. 1 is plotted the invariant cross section $d^2\sigma / V_\perp dV_{//} dV_\perp$ in the velocity plane for LCP's and IMF's and for different impact parameter bins. These data have been obtained in the collisions of 79 MeV per nucleon ^{64}Zn on ^{nat}Ti . Similar trends are observed at other bombarding energies and with the $^{36}Ar + ^{27}Al$ system as well. For all particles and IMF's a high velocity source is seen whose mean value decreases with the decrease of the impact parameter b_{EXP} . For Z=1 and Z=2 particles, a low velocity component appears. This target-like component is not seen with IMF's as the experimental thresholds prevent their detection. A third component shows up at half the beam velocity, mainly with LCP's of Z=1 and to a lesser extent with LCP's of Z=2 and IMF's : this component comes from pre-equilibrium particles which escape from the system very early after they have undergone nucleon-nucleon collisions in the interaction zone between projectile and target.

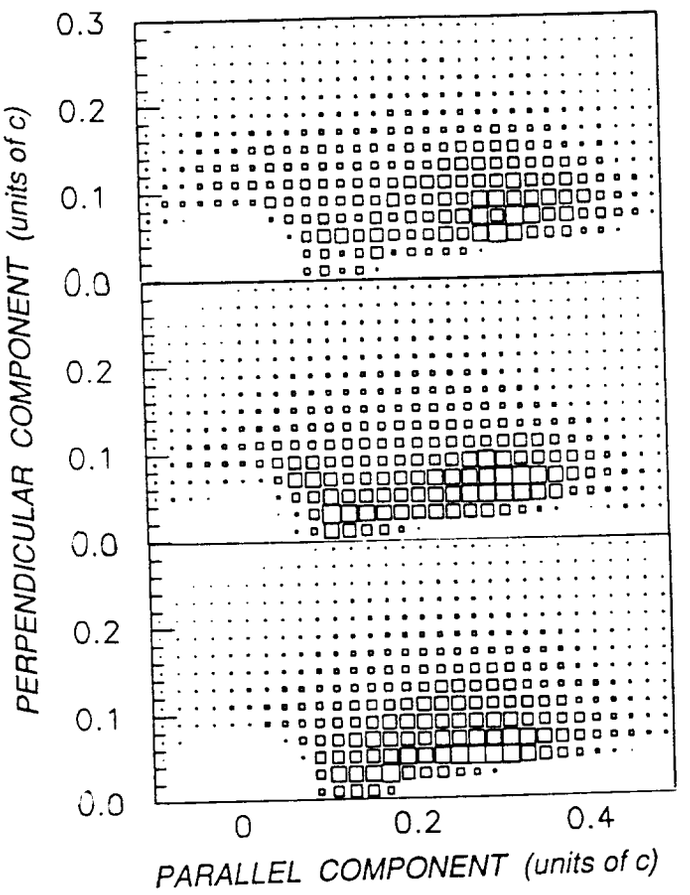

Fig. 2 : Invariant cross-sections $d^2\sigma / V_\perp dV_\perp dV_{//}$ for Z=1 particles and experimental impact parameters in between 0 and 2 fm. Top : QMD calculations, middle : experimental data, bottom : EUGENE calculations.

These observations are compatible with dissipative binary collisions accompanied by a sizeable pre-equilibrium emission. These characteristics are well reproduced by statistical calculations using the EUGENE code [13] and dynamical calculations performed with the QMD model [14] (see fig. 2). An overall agreement is established between data and calculations in which only collisions leading to two main fragments are predicted to occur. In particular, the enhancement of the mean transverse momentum of LCP's at mid-rapidity is accounted for [15].

At lower bombarding energies, a fraction of the cross section can be attributed to a fusion-like mechanism. Residues with large masses and velocity close to the center of mass velocity have been observed in the 35 MeV per nucleon ^{64}Zn + ^{nat}Ti. They correspond to a cross section of ~ 150 mb [16]. This value is less than 25 mb at 49 MeV per nucleon.

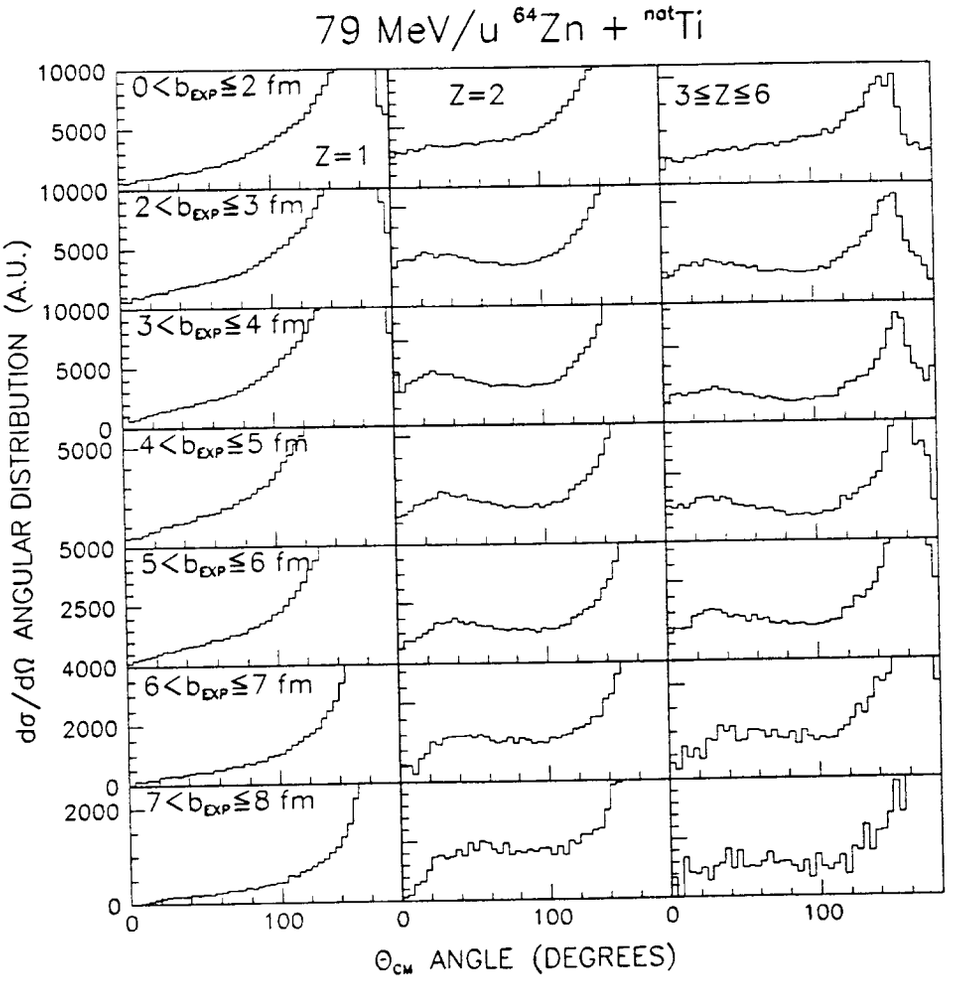

Fig. 3 : Angular distributions in the frame of the source for Z=1 (left), Z=2 (middle), and 3≤Z≤6 (right) and for different experimental impact parameter bins. These data are from the 79 MeV per nucleon ^{64}Zn + ^{nat}Ti reactions.

4 - CHARACTERISTICS OF HOT NUCLEI

In this section, we will concentrate on the determination of the characteristics of hot nuclei associated with the fast source seen in fig. 1. First we will look at the angular distributions of LCP's and IMF's in the frame of the hot nucleus, then we will calculate both the mass and excitation energy of the primary hot nucleus.

4.1. Angular distributions of LCP's and IMF's

In fig. 3, are shown the angular distributions of LCP's and IMF's in the frame of the hot nucleus as a function of the impact parameter b_{EXP}. For that purpose, the source velocity has been calculated in two ways which lead to similar results. Either the centroid of the parallel velocity distribution of fragments with $Z \geq 6$ has been taken, in each impact parameter bin, or the source velocity vector was reconstructed, for each event, from the momenta of all particles with $Z \geq 2$ and velocity larger than the center of mass velocity [15]. Most of the angular distributions exhibit the same behaviour, with a plateau at forward angles and a marked peak at backward angles. This peak comes from the addition of particles emitted by both the projectile-like and target-like fragments. This backward contribution is even more pronounced with the Z=1 particles due to the pre-equilibrium component. From these angular distributions a clear isotropic emission of Z=2 particles and IMF's is evidenced. Although such a pattern is not seen with the Z=1 particles and it is actually worsened by the non identification of protons below 10° in the laboratory system, we assume that all LCP's and IMF's emitted in the forward hemisphere in the frame of the hot nucleus are de-excitation products of that hot nucleus. Therefore the characteristics of the hot nucleus can be deduced by taking twice the contribution of the forward emitted decay products.

4.2. Primary mass distribution

The primary charge of the hot nucleus is reconstructed by adding to the charge of the largest fragment twice the sum of all charges detected in the forward hemisphere in its own frame. The mass is obtained assuming the A/Z ratio of the projectile.

In figs. 4 and 5 are displayed the masses of the largest fragment and of the reconstructed hot nucleus for the $^{64}Zn + {}^{nat}Ti$ and $^{36}Ar + {}^{27}Al$ reactions as a function of b_{EXP} and for different bombarding energies, respectively. The mass of the largest fragment strongly decreases with the decrease of the impact parameter. This is consistent with an increase of the excitation energy deposit in the projectile like fragment when going from peripheral to central collisions. For a given impact parameter, a decrease of the mass when the bombarding energy increases is also seen, meaning that higher excitation energies are deposited when increasing the bombarding energy.

In constrast with the evolution of the mass of the largest fragment, the reconstructed mass of the hot nuclear source, shown in figs. 4 and 5, does not evolve with the impact parameter or the bombarding energy. A rather constant mass value slightly lower than the projectile mass comes out.

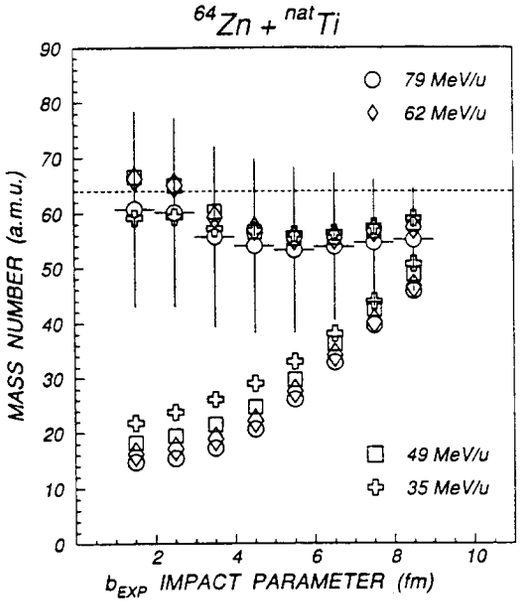

Fig. 4 : Masses of the largest fragment (lower symbols) and of the reconstructed primary hot nucleus (upper symbols), measured in the $^{64}Zn+^{nat}Ti$ reactions, as a function of the experimental impact parameter and for different bombarding energies.

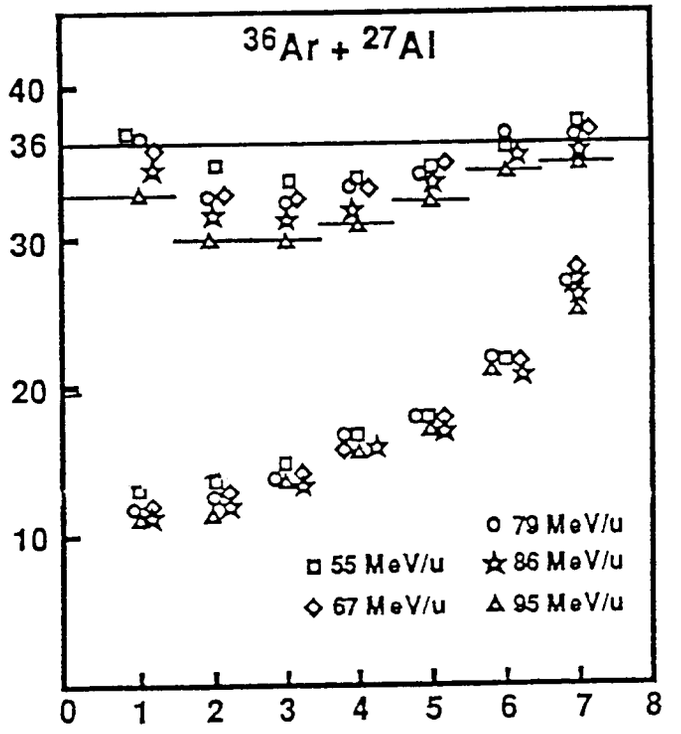

Fig. 5 : Same as fig. 4 for the $^{36}Ar+^{27}Al$ reactions.

However we have to mention that these mass values are upper limits since pre-equilibrium particles emitted in the forward hemisphere in the frame of the hot nucleus are taken into account and lead to an overestimation of the reconstructed mass. Attempts were made in order to estimate the pre-equilibrium contribution using both the EUGENE and QMD models. This overestimation increases with the decrease of the impact parameter b_{EXP}, reaching 15 % in the central collisions.

4.3. Excitation energy distribution

The excitation energy of the hot nucleus is deduced in an event by event basis from the kinetic energies of all its decay products [10] :

$$E^* = T_{LF} + 2 \sum_{i=1}^{\nu_c} T_i + \sum_{j=1}^{\nu_n} T_j - Q$$

In the above expression T_i represents the kinetic energy of the i^{th} charged particle emitted in the forward hemisphere in the frame of the hot nucleus, T_j the kinetic energy of the j^{th} evaporated neutron and Q is the energy difference between the initial and final masses. The multiplicity of neutrons, not detected in the experiments, is calculated from the difference between the mass of the primary hot nucleus and the sum of all detected masses issued from the hot nucleus. Each neutron has been given a mean kinetic energy equal to twice an effective temperature taken as $T_{eff} = 3/4\ T_{INIT}$ in order to account for the decay chain, with $E^* = a\ T^2_{INIT}$ and a the level density parameter ($a = A / 8\ MeV^{-1}$).

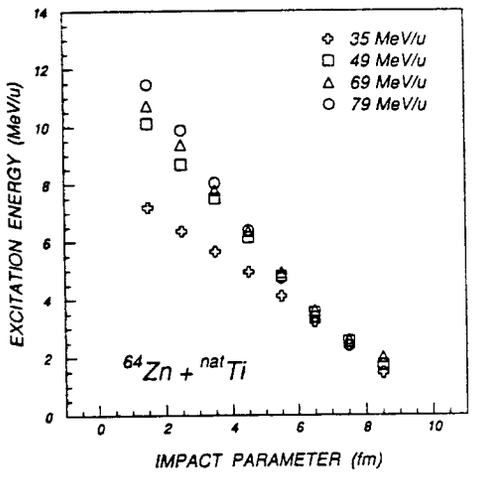

Fig. 6 : Mean values of the excitation energy distributions of hot nuclei formed in the $^{64}Zn+^{nat}Ti$ reactions, as a function of the experimental impact parameter and for different bombarding energies.

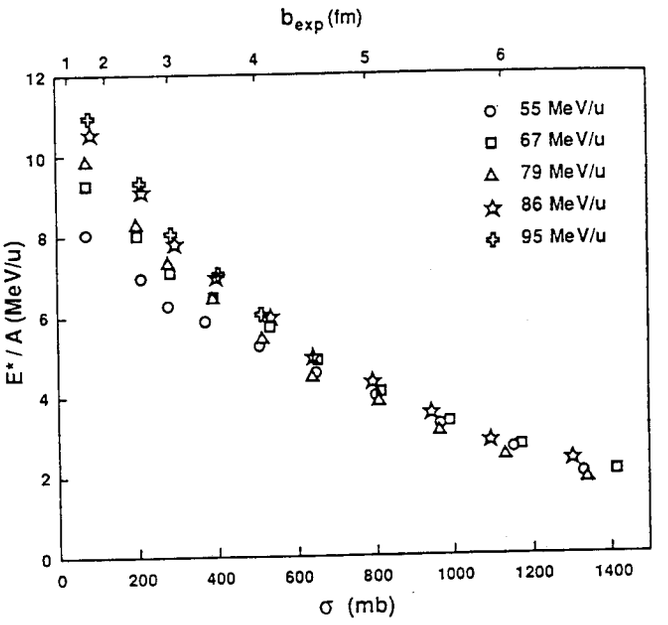

Fig. 7 : Same as fig. 5 for the $^{36}Ar+^{27}Al$ reactions.

The excitation energies so derived are drawn in figs. 6 and 7 as a function of the impact parameter b_{EXP} and for different bombarding energies. The excitation energy grows up when the impact parameter decreases. For a given b_{EXP} , the excitation energy rises up with the bombarding energy as mentioned in sect. 4.2. Very high excitation energies are reached in the most central collisions, between 10 and 12 MeV per nucleon in the $^{64}Zn + ^{nat}Ti$ system and between 9 and 11 MeV per nucleon in the $^{36}Ar + ^{27}Al$ system.

The remark done in sect. 4.2. about the primary masses stands also for the excitation energies. They also represent upper limits. The EUGENE code indicates an overestimation of the excitation energy by ~15% in the most central collisions. Nevertheless, when this correction due to the pre-equilibrium contribution is taken into account, very high excitation energies of the order of 10 MeV per nucleon are still observed.

5 - CONFRONTATION OF THE DATA WITH THEORETICAL PREDICTIONS

In the previous sections, the characteristics of the hot nuclear sources, i.e. their mass and excitation energy distributions, have been extracted from the experiments and studied as a function of the impact parameter b_{EXP} and of the bombarding energy. In order to gain insight into the mechanisms of formation and decay modes of these hot nuclei, comparisons have been performed using three theoretical models.

5.1. *Theoretical models*

The two first models are the statistical code EUGENE [13] and the dynamical code QMD [14] which both follow the entire evolution of the collision, while the third one, the statistical model WIX [17], simulates the desintegration of one single source.

The event generator EUGENE is a two-step model [13]. In the entrance channel, the nucleons belonging to the overlapping interaction zone between projectile and target undergo nucleon-nucleon collisions and either they escape from the composite system, leading to the pre-equilibrium component, or they are trapped in the receptor nuclei while their kinetic energy is converted into intrinsic excitation energy. In the exit channel, the excited nuclei undergo sequential decay by fission or evaporation of LCP's and IMF's, both mechanisms being described in a unified way taking into account their dynamical competition.

The quantum-molecular dynamics model [14] is a n-body theory which simulates heavy-ion collisions at intermediate energies. The nucleons are represented by gaussian wave functions in momentum and coordinate space and interact via a mean field replaced by two and three body interactions, as well as via two body collisions. The time evolution of the collision is followed till 200 fm/c . At that time, cluster formation occurs : all nucleons being closer than 3 fm from each other in the coordinate space are considered members of the same cluster. After cluster formation is completed, all clusters are practically cold nuclei.

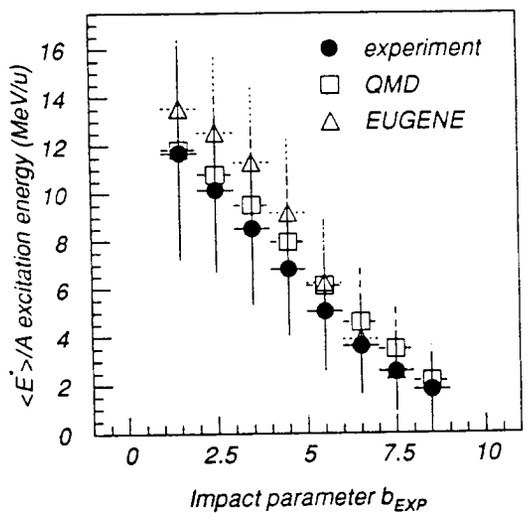

Fig. 8 : Mean values and standard deviations of the excitation energy distribution of hot nuclei formed in the 79 MeV per nucleon $^{64}Zn+^{nat}Ti$ reactions. The data (closed circles) are compared to EUGENE calculations [13] (open triangles) and to QMD calculations [14] (open squares).

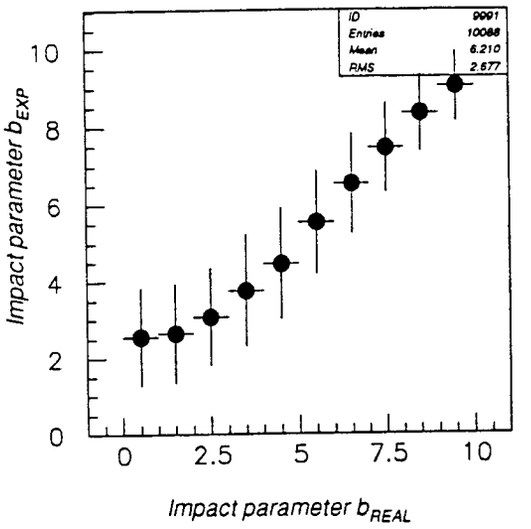

Fig. 9 : Correlation, calculated in the QMD model [14], between the real impact parameter b_{REAL} and the impact parameter b_{EXP} deduced as in the experiment (see sect. 2.2.).

The WIX code [17] is an extension of the earlier statistical event generator FREESCO [18] with which, according to the amount of excitation energy, a nucleus either deexcites by standard sequential evaporation of light particles or undergoes an explosive transformation into excited fragments (these fragments subsequently deexcite by evaporation of light particles). To this basic model the following important new features have been incorporated : the Coulomb interaction between fragments is explicitely treated as well as the construction of the freezeout configuration, part of the excitation energy may be associated with a collective expansion and the source may be both deformed and hollow. Of peculiar interest is the possibility that a fraction of the total excitation energy be stored in a collective radial flow component. In that case, less thermal energy is available, more fragments are produced and the corresponding kinetic energy spectra grow harder since the collective energy is proportional to the mass while the statistical energy is independent of the mass.

5.2. Excitation energy distributions

The excitation energies measured in the 79 MeV per nucleon $^{64}Zn + ^{nat}Ti$ reactions are shown in fig. 8 together with the results of the EUGENE and QMD calculations. The theoretical predictions have been filtered by the acceptance of the experimental set-up and analyzed in the same way as the data. In particular, the real impact parameter of the models have been disregarded. Instead, an experimental impact parameter deduced, as in the experiment, from the total transverse momentum has been used (cf. sect. 2.1.). The correlation between the real and the experimental impact parameter is displayed in fig. 9. An excellent agreement is obtained at high bombarding energies but the correlation worsens at lower bombarding energies [16, 19].

In fig. 8, the QMD calculations reproduce the experiment in a very satisfactory way, while the EUGENE calculations overpredict the excitation energies by 2 MeV per nucleon in the central collisions.

In the following we will concentrate on the hotest nuclei, those associated with an experimental impact parameter in between 0 and 2 fermis, corresponding to a cross-section of 125 mb and an excitation energy of 11 - 12 MeV per nucleon. We will look first at the multiplicity distribution of LCP's and IMF's emitted by these very hot nuclei and then at the kinetic energy spectra of these particles.

5.3. Multiplicities

The multiplicity distributions of LCP's and IMF's are compared to theoretical predictions in fig. 10. The QMD calculations (upper row in fig. 10) overestimate the yield of hydrogen nuclei and predicts a too small number of both the helium nuclei and IMF's by almost a factor of 2 . A too high number of Z=1 is calculated by the EUGENE code (middle row in fig. 10), while the multiplicity of Z=2 is very well reproduced. Consequently, too few IMF's are predicted. On the other hand, a very good agreement is obtained with the WIX model, in which an isotropic collective expansion has been introduced (lower row in fig. 10). When the collective expansion is switched off, more thermal energy is available, leading to prefragments with higher excitation energy and, as a result, to a more abundant emission of LCP's, especially of Z=1 particles.

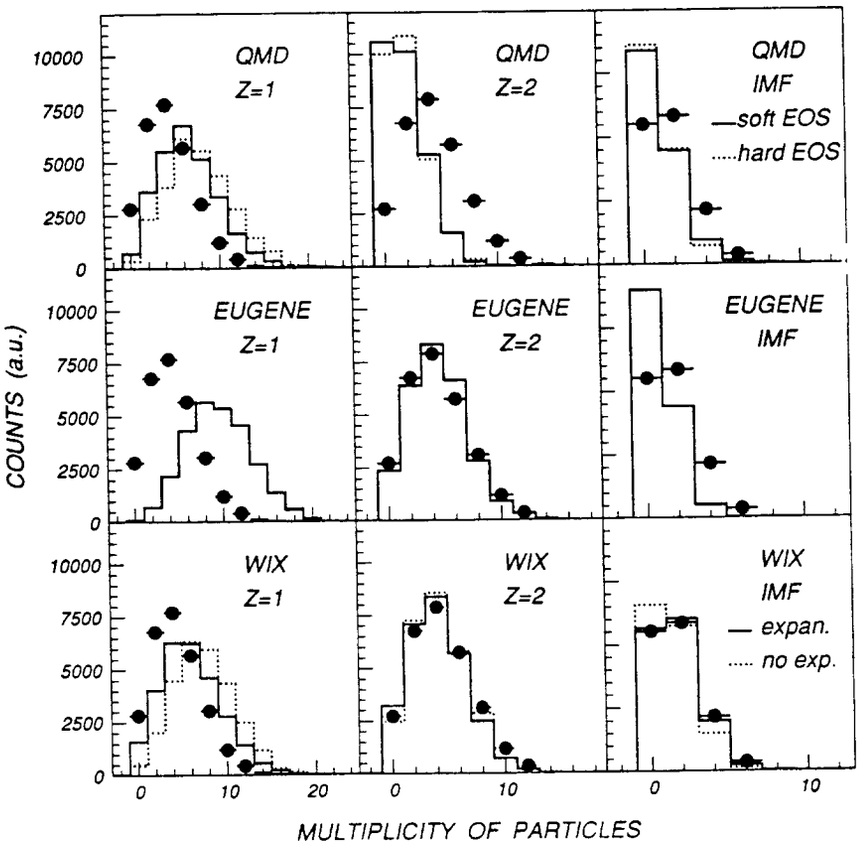

Fig. 10 : Multiplicity distributions of Z=1, Z=2 and IMF's (3≤Z≤8) emitted by the hot nuclei formed in the most central collisions in the 79 MeV per nucleon $^{64}Zn+^{nat}Ti$ reactions. They are compared to theoretical predictions : QMD with a soft equation of state (solid lines) and a hard equation of state (dotted lines) [14] (upper row), EUGENE [13] (middle row) and WIX with a collective expansion of 2.7 MeV per nucleon (solid lines) and no expansion (dotted lines) [17] (lower row).

5.4. Kinetic energy spectra

In fig. 11 are shown the kinetic energy spectra for LCP's and IMF's with Z=3, 4 and 5 , respectively. These spectra have been integrated between 30 and 60° in the frame of the hot nucleus. While the hydrogen and helium spectra are compatible with a thermal scenario, as indicated by the comparison of the data with the prediction of the statistical codes EUGENE and WIX (with Coulomb interaction and no expansion), the kinetic energy spectra of IMF's exhibit a high energy tail which cannot be explained by the sole thermal emission of a hot source. Indeed, an additional component is needed to boost the IMF's with larger velocities. The kinetic energy spectra of Z=1 and 2 are not modified when a part of the total energy goes into a collective expansion, because, for these LCP's, the collective radial energy which is proportional to the mass, remains small as compared to the thermal energy which is independent of the mass. On the other hand, the collective energy grows up with the increase of the mass of IMF's and significant alterations of the kinetic energy spectra are observed. As seen in fig. 11, the spectral shapes of IMF's are well reproduced when assuming a collective expansion of 2.7 MeV per nucleon (see sect. 5.5). The QMD calculations look like

identical to statistical calculations without collective expansion. In fig. 11 are drawn the results obtained with both a soft (K=200 MeV) and a hard (K=380 MeV) equation of state. Using a higher K compressibility modulus leads to higher mean values of the kinetic energy spectra by more than 2 MeV per nucleon for LCP's and less than 1 MeV per nucleon for IMF's.

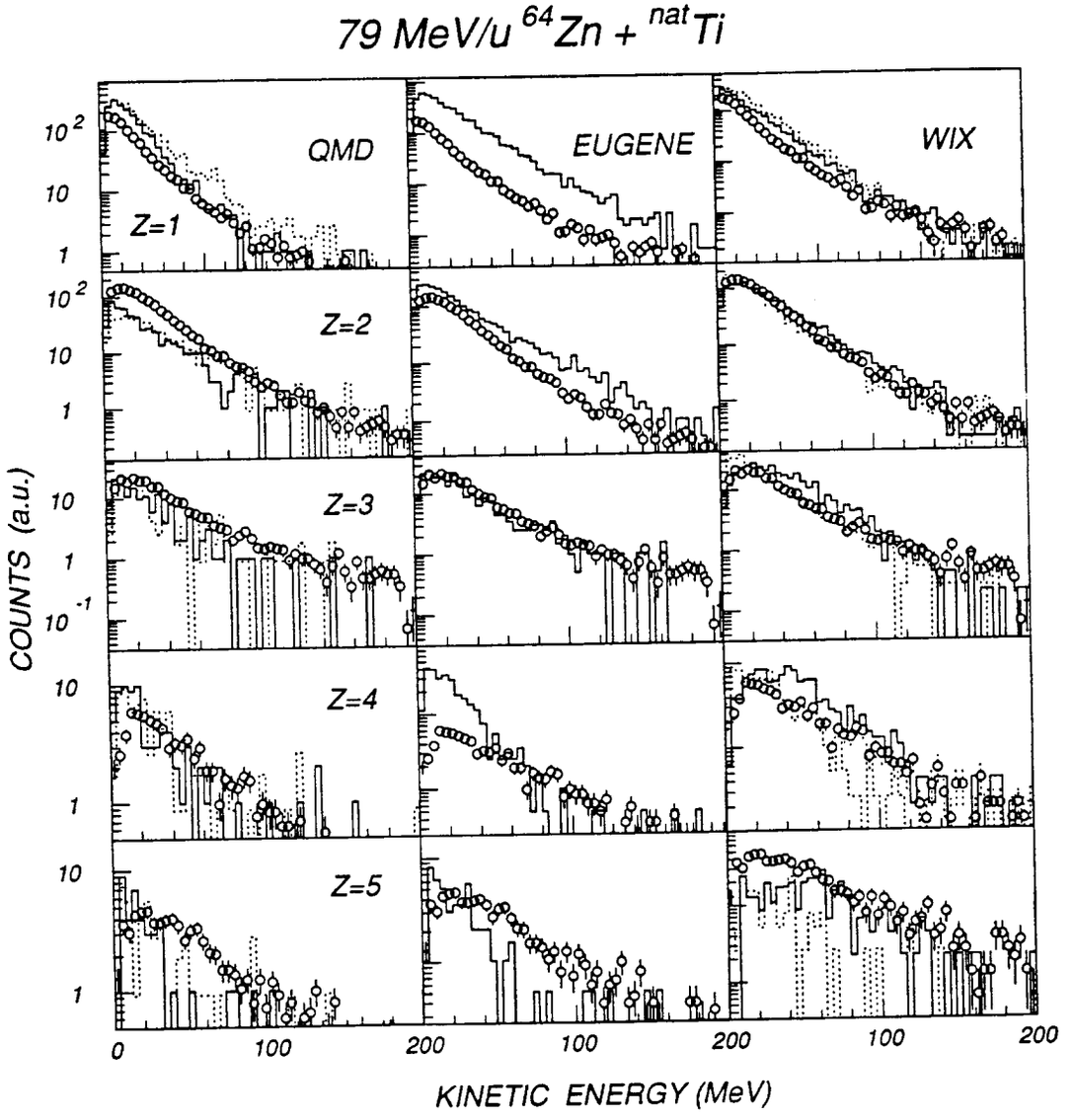

Fig. 11 : Kinetic energy spectra of particles with atomic number ranging from 1 up to 5 , emitted by the hot nuclei formed in the most central collisions in the 79 MeV per nucleon $^{64}Zn+^{nat}Ti$ reactions. The kinetic energy spectra have been integrated between 30 and 60° in the frame of the hot nucleus. They are compared with theoretical calculations : (see legend of fig. 10).

5.5. *Mean values of the kinetic energy spectra*

In fig. 12, the mean value per nucleon of the kinetic energy spectra of LCP's and IMF's are shown as a function of the fragment charge. The data (closed circles) are compared to the predictions of theoretical models. The statistical calculations performed with EUGENE (open circles) and with WIX without a collective expansion (open stars) as well as the QMD dynamical calculations (open crosses) fail at reproducing the experimental values. For IMF's with charge greater than 3, an underestimation by more than 2 MeV per nucleon is observed. On the other hand, when an isotropic collective expansion is accounted for in the WIX model (open squares), a better agreement is obtained with the data. A more detailed comparison of the data with the predictions of the WIX model are shown in fig. 13. As seen, the data are well accounted for when considering an isotropic collective expansion in between 1.8 and 2.7 MeV per nucleon. We did not try to fit the experimental data to extract a precise value of the expansion. The aim of that comparison is to derive the magnitude of the collective radial flow with respect to the available kinetic energy in the center of mass and to the excitation energy of the hot nucleus. From fig. 13, a collective expansion of 2. - 2.5 MeV per nucleon is deduced and no clear evolution of this expansion is observed as a function of the fragment charge at variance with ref. [8]. Except the hydrogen nuclei for which the mean value is slightly overestimated, the helium nuclei and IMF's seem to participate equally in the collective expansion. The value of 2. - 2.5 MeV per nucleon corresponds to 10-15% of the total kinetic energy available in the center of mass of the reaction and to 20% of the total excitation energy of the hot nucleus.

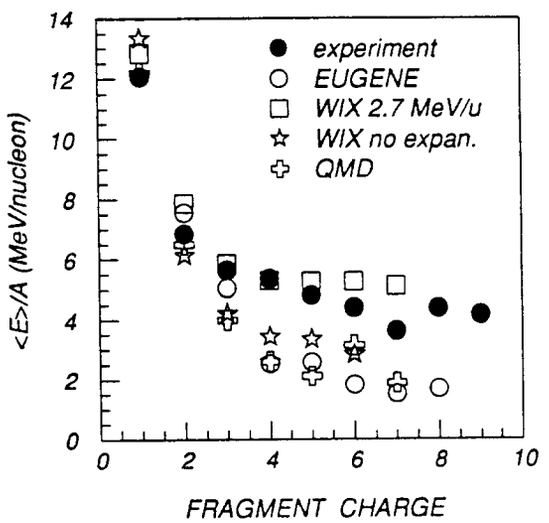

Fig. 12 : Mean value of the kinetic energy spectra as a function of the fragment charge, for the most central collisions in the 79 MeV per nucleon $^{64}Zn+^{nat}Ti$ reactions.

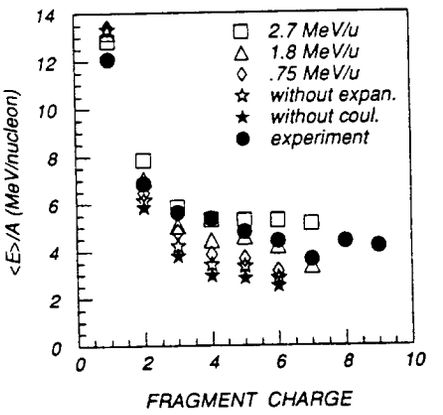

Fig. 13 : Same as fig. 12. The data (closed symbols) are compared to WIX calculations [17] : no coulomb interaction and no expansion (closed stars), with coulomb interaction and no expansion (open stars), with coulomb interaction and different values of the collective expansion, 0.75, 1.8 and 2.7 MeV per nucleon (open diamonds, open triangles and open squares, respectively).

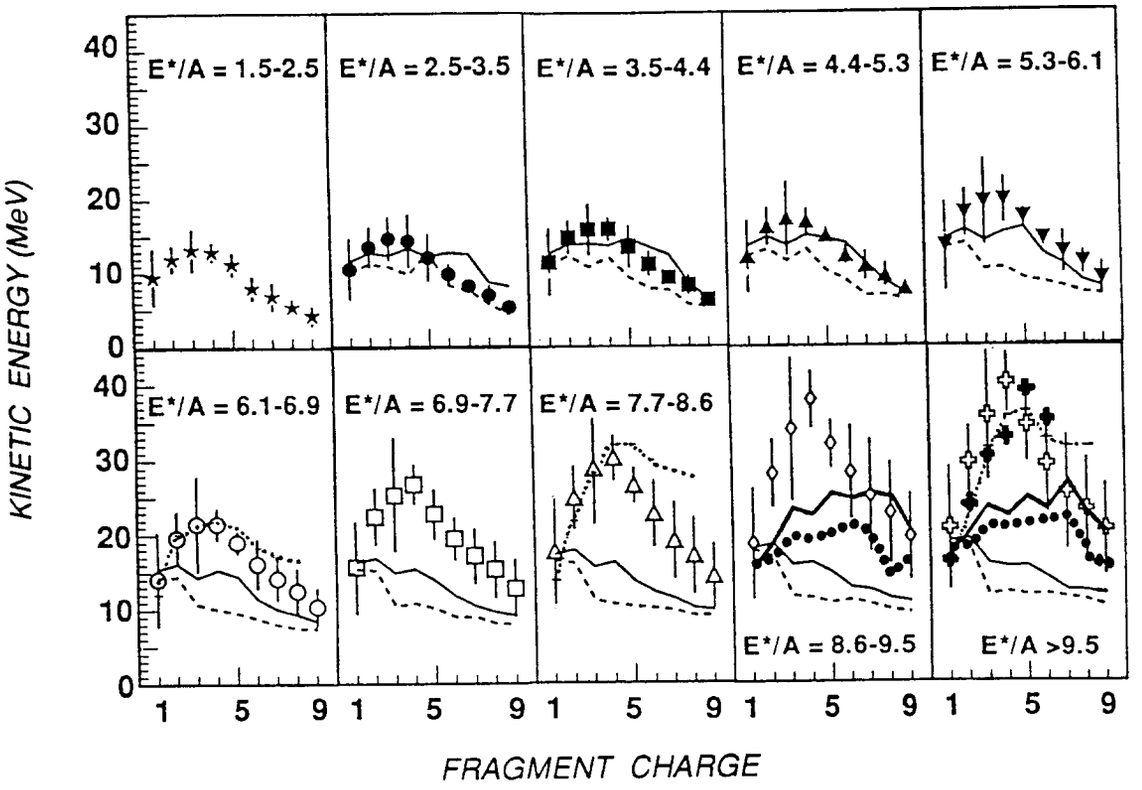

Fig. 14 : Mean values and standard deviations of the kinetic energy spectra of hot nuclei formed in the $^{36}Ar+^{27}Al$ reactions at bombarding energies ranging from 55 to 95 MeV per nucleon, as a function of the fragment charge and for various excitation energy bins. These values have been corrected from the pre-equilibrium component. They are compared to calculations of EUGENE [13] (see text) and WIX [17] : without collective expansion (thick dotted lines) and expansion of 0.9 and 1.8 MeV per nucleon (thick line and closed crosses, respectively).

In fig. 14, similar data concerning the $^{36}Ar + ^{27}Al$ system are plotted as a function of the deposited excitation energy. For the sake of statistics data corresponding to different bombarding energies and to the same excitation energy bin have been summed up after it was checked that for a given excitation energy bin, the mean value of the kinetic energy spectra does not evolve significantly as a function of the bombarding energy [15]. Thin solid and dashed lines drawn in fig. 14 represent statistical sequential calculations carried out with the EUGENE code using two different prescriptions for the level density parameter (a = A/13 and expression from [20], respectively). These predictions account for excitation energies less than 5-6 MeV per nucleon and fail at reproducing the higher excitation energies. A modified version of the EUGENE code starting with a freeze-out configuration of the decaying hot nucleus and allowing for a collective radial expansion of the source leads to results in better agreement with the data. Such an expansion is clearly needed in order to reproduce the data, the value of which is seen to increase with the increase of the excitation energy (thin dotted lines in fig. 14). At ~ 6.5 MeV per nucleon, an isotropic radial flow of .5 MeV per nucleon brings the calculations at the level of the experimental data and ~ 1.5 MeV per nucleon is needed at ~ 8 MeV

per nucleon of excitation energy. However, for the hotest nuclei, with excitation energy higher than 9.5 MeV per nucleon, a unique value of the radial flow does not describe all the data. Calculations performed with EUGENE (WIX) with an expansion of 2.0 (1.8) MeV per nucleon, shown as thin dotted line (closed crosses) in the lower right hand part in fig. 14, give only a quantitative description of the data. Clearly a higher value of the radial flow is needed for LCP's and the lightest IMF's while a lower value is needed for the heaviest IMF's.

6 - DISCUSSION

Are the hot nuclei studied in this paper equilibrated nuclei ? As seen in sect. 4.1., these nuclei decay by an isotropic emission of LCP's and IMF's. Furthermore both the multiplicities of emitted particles and their kinetic energy spectra are well accounted for by a statistical multifragmentation model. The success of such a description gives a strong support for the assumption of a primary hot nucleus whose excitation energy has been equilibrated. However, further dynamical calculations should be carried out before concluding about the validity of global thermodynamical concepts to such hot nuclei.

Concerning the question of a radial flow component, a few experimental results become available in the literature. In the Ca+Ca system studied at 35 MeV per nucleon [21], it has been shown that an expansion energy of 0.75 to 1.0 MeV per nucleon in the framework of the EES model [5] was needed in order to reconcile both the data and calculations. A somewhat higher value has been extracted from the similar system $^{32}S+^{27}Al$ measured at 37.5 MeV per nucleon [7], while no significant radial flow comes out from the measurements of the 50 MeV per nucleon Xe + Sn reactions [22]. At higher bombarding energies and for the very heavy Au+Au system [6, 8], it was found, in central collision events, that the kinetic energy of LCP's and IMF's is essentially dominated by the collective motion of the outstreaming matter, with a slight dependence as a function of the charge of the emitted particles. Our analyses lead to results in between those obtained at 30-40 MeV per nucleon and those obtained above 100 MeV per nucleon. The data argue in favour of an increasing collective expansion energy with the excitation energy. This collective component starts at an excitation energy value of the order of 6 MeV per nucleon.

The exact nature of the mechanism responsible for the formation of the hot nuclei studied in this paper is not yet very well established : is there formation of a hot participant zone whose escaping energetic nucleons transfer their kinetic energy in excitation energy into the spectator nuclei, or is there any transparency effect between projectile and target as indicated in Landau-Vlasov calculations [23] ? On the other hand, their decay seems to be better understood. After an initial compression, the hot nuclear system expands towards low density regions. Values of 1/2 to 1/3 ρo are usually derived from models [3, 17]. While expanding, the hot nuclear system breaks up isotropically into IMF's (eventually excited) and LCP's.

7 - CONCLUSION

We studied the decay properties of hot nuclei produced in the $^{64}Zn+^{nat}Ti$ reactions between 35 and 79 MeV per nucleon and the $^{36}Ar+^{27}Al$ reactions between 55 and 95 MeV per nucleon. Only well detected events were kept in the analysis. Most of the collisions lead to the formation of two main products accompanied by an emission of LCP's centered at mid-rapidity. Use of the total transverse momentum has been done to sort the events as a function of the impact parameter. The mass and excitation energy of the fast source were determined. These hot nuclei decay by an isotropic emission of LCP's and IMF's. Very high excitation energy values (more than 10 MeV per nucleon) are reached in central collisions and for the highest bombarding energies. The $^{64}Zn+^{nat}Ti$ data have been confronted to the predictions of several calculations. These calculations were filtered by the acceptance of the experimental set-up and analyzed in the same way as the data. All calculations agree in reproducing the general features of the data : primary mass and excitation energy distributions. A closer inspection to the multiplicity of LCP's and IMF's emitted by the hotest nuclei, as well as to their kinetic energy spectra, reveals that only the statistical emission from a hot source, in which a collective expansion has been included, is able to account, with an excellent agreement, for the data associated with the most violent collisions. From this comparison, a collective energy of 2 to 2.5 MeV per nucleon has been derived. It represents a fraction of 20% of the total excitation energy. Similar statements are deduced from the analysis of the $^{36}Ar + ^{27}Al$ reactions, for which a gradual increase of the collective expansion is seen with the increase of the excitation energy above ~6 MeV per nucleon.

REFERENCES

[1] J. Aichelin and H. Stöcker, Phys. Lett. B176 (1986) 14

[2] B. Remaud et al, Nucl. Phys. A488 (1988) 423c

[3] E. Suraud et al, Phys. Lett. B229 (1989) 359

[4] L. Vinet et al, Nucl. Phys. A468 (1987) 321

[5] W.A. Friedman, Phys. Rev. C42 (1990) 667

[6] S.C. Jeong et al, Phys. Rev. Lett. 72 (1994) 3468

[7] D. Heuer et al, Phys. Rev. C50 (1994) 1943

[8] W.C. Hsi et al, Phys. Rev. Lett. 73 (1994) 3367

[9] D. Cussol et al, Proceedings of the XXXI International Winter Meeting on Nuclear Physics, Bormio, Italy, 1993, p. 250

[10] D. Cussol et al, Nucl. Phys. A561 (1993) 298

[11] G. Bizard et al, Nucl. Instr. and Meth. A244 (1986) 483

[12] A. Péghaire et al, Nucl. Instr. and Meth. A295 (1990) 365

[13] D. Durand, Nucl. Phys. A541 (1992) 266

[14] J. Aichelin, Phys. Rep. 202 (1991) 233

[15] S.C. Jeong et al, in preparation

[16] A. Kerambrun et al, internal report LPCC 94-14 and in preparation

[17] J. Randrup, Comp. Phys. Comm. 77 (1993) 153

[18] G. Fai and J. Randrup, Comp. Phys. Comm. 42 (1986) 385

[19] R. Wada et al, "Progress in Research" report, Texas A&M University, 1994, p. I29

[20] C. Guet et al, Phys. Lett. B205 (1988) 427

[21] K. Hagel et al, Phys. Rev. Lett. 68 (1992) 2141 and report TAMU 94-08

[22] V. Métivier et al, this conference

[23] E. de Filippo et al, this conference